AEM
Journals.ASM.org

Distribution, Activities, and Interactions of Methanogens and Sulfate-Reducing Prokaryotes in the Florida Everglades

Hee-Sung Bae,[a] M. Elizabeth Holmes,[b] Jeffrey P. Chanton,[b] K. Ramesh Reddy,[a] Andrew Ogram[a]

Soil and Water Science Department, University of Florida, Gainesville, Florida, USA[a]; Department of Earth, Ocean, & Atmospheric Science, Florida State University, Tallahassee, Florida, USA[b]

To gain insight into the mechanisms controlling methanogenic pathways in the Florida Everglades, the distribution and functional activities of methanogens and sulfate-reducing prokaryotes (SRPs) were investigated in soils (0 to 2 or 0 to 4 cm depth) across the well-documented nutrient gradient in the water conservation areas (WCAs) caused by runoff from the adjacent Everglades Agricultural Area. The methyl coenzyme M reductase gene (*mcrA*) sequences that were retrieved from WCA-2A, an area with relatively high concentrations of SO_4^{2-} (≥39 μM), indicated that methanogens inhabiting this area were broadly distributed within the orders *Methanomicrobiales*, *Methanosarcinales*, *Methanocellales*, *Methanobacteriales*, and *Methanomassiliicoccales*. In more than 3 years of monitoring, quantitative PCR (qPCR) using newly designed group-specific primers revealed that the hydrogenotrophic *Methanomicrobiales* were more numerous than the *Methanosaetaceae* obligatory acetotrophs in SO_4^{2-}-rich areas of WCA-2A, while the *Methanosaetaceae* were dominant over the *Methanomicrobiales* in WCA-3A (with relatively low SO_4^{2-} concentrations; ≤4 μM). qPCR of *dsrB* sequences also indicated that SRPs are present at greater numbers than methanogens in the WCAs. In an incubation study with WCA-2A soils, addition of MoO_4^{2-} (a specific inhibitor of SRP activity) resulted in increased methane production rates, lower apparent fractionation factors [α_{app}; defined as (amount of $\delta^{13}CO_2$ + 1,000)/(amount of $\delta^{13}CH_4$ + 1,000)], and higher *Methanosaetaceae mcrA* transcript levels compared to those for the controls without MoO_4^{2-}. These results indicate that SRPs play crucial roles in controlling methanogenic pathways and in shaping the structures of methanogen assemblages as a function of position along the nutrient gradient.

The Florida Everglades is a large freshwater subtropical wetland at the southern end of the Florida peninsula (see Fig. S1 in the supplemental material), and it was estimated to harbor at one time the largest single body of organic soils in the world, covering over 8,000 km^2 (1). Wetlands, including the Everglades, are the primary source of natural global CH_4 emissions, producing more than 150 Tg of CH_4 annually (roughly 20% of global annual emissions) (2, 3). The Everglades ecosystem was historically limited in nutrients, particularly phosphorus (P); however, the discharge of agricultural drainage from the adjacent Everglades Agricultural Area (EAA) led to elevated nutrient levels in the northern Everglades, particularly in Water Conservation Area 2A (WCA-2A), which is characterized by a well-documented gradient in soil and water P concentrations (4–7). The alleviation of P limitation resulted in many changes to the WCA-2A ecosystem; primary productivity was significantly increased, and the dominant plant species changed from saw grass to cattail. In addition, organic matter mineralization to CO_2 and CH_4 was greatly increased (8, 9).

Numerous studies on the impacts of nutrient additions to WCA-2A soils have been conducted, including analyses of methanogen community structures (10–12) and methanogenesis rates (8, 9). However, the detailed mechanisms controlling methanogenic pathways and the development of methanogenic guilds in response to shifting nutrient limitations are poorly understood.

In freshwater wetlands, CH_4 is primarily produced via two pathways: hydrogenotrophic methanogenesis (HM; $CO_2 + 4H_2 \rightarrow CH_4 + 2H_2O$) and acetoclastic methanogenesis (AM; $CH_3COOH \rightarrow CH_4 + CO_2$). From the stoichiometry of glucose fermentation, the relative proportions of the two pathways are 33% HM and 67% AM (13). The natural distribution of the two pathways generally follows this proportion; however, some notable exceptions have been reported in the literature. Recent work (14) indicated that the relative contributions of the methanogenic pathways in WCA-2A may be related to nutrient status in the Everglades; relatively greater HM is observed in nutrient-impacted soils, and the predicted proportions are observed in nutrient-unimpacted soils.

Various factors have been suggested to be responsible for those cases in which the relative contributions of the HM and AM pathways deviate significantly from those predicted by stoichiometry, including soil depth (15, 16), nutrient type (17), seasonal conditions (18), pH (19, 20), and vegetation type (21). However, competition between methanogens and other functional groups of microorganisms has not been extensively studied as a possible mechanism responsible for shifts in the relative proportions of HM versus AM pathways. Methanogens and microorganisms that use more energy-yielding alternative terminal electron acceptors, such as SO_4^{2-}, Fe(III), NO_3^-, or O_2, may compete for substrates such as acetate and H_2.

Competition between sulfate-reducing prokaryotes (SRPs)

Received 13 May 2015 **Accepted** 7 August 2015

Accepted manuscript posted online 14 August 2015

Citation Bae H-S, Holmes ME, Chanton JP, Reddy KR, Ogram A. 2015. Distribution, activities, and interactions of methanogens and sulfate-reducing prokaryotes in the Florida Everglades. Appl Environ Microbiol 81:7431–7442. doi:10.1128/AEM.01583-15.

Editor: G. Voordouw

Address correspondence to Andrew Ogram, aogram@ufl.edu.

Supplemental material for this article may be found at http://dx.doi.org/10.1128/AEM.01583-15.

and methanogens for the common substrates acetate and H_2 has been well documented in various environments, including marine sediments (22, 23), freshwater sediments (24, 25), and bioreactors (26); however, little attention has been given to the possibility that this competition may impact the dominant methanogenic pathway. The interactions between SRPs and methanogens may be complex, depending on the availability of both electron donors and electron acceptors. The interaction may be competitive when sufficient sulfate is available to serve as a terminal electron acceptor for SRPs; however, it may be more likely to be cooperative via a syntrophic relationship when SO_4^{2-} is limiting (27, 28). SO_4^{2-} has been recognized to be an important contaminant in the northern water conservation areas (WCAs) (29). Hence, the SRP-methanogen interaction may be a crucial factor determining the methanogenic pathway in the WCAs.

The objective of this research was to determine the distribution and population dynamics of methanogens and SRPs across nutrient gradients in WCAs and to evaluate the potential interactions between SRPs and methanogens as a driving force shaping methanogenic community structures and pathways. For this study, we selected sites distinct from each other with respect to the concentrations of P and SO_4^{2-}, key geochemical parameters that have been shown to affect methanogenesis and SO_4^{2-} reduction in Everglades wetland soils (9, 10, 29). This study extends our knowledge of the mechanisms related to methane production and of the interplay between methanogens and SRPs in freshwater wetlands.

MATERIALS AND METHODS

Sampling and sample processing. Replicate soil cores (≥3 cores for each site within approximately 25 m^2) were obtained from sites F1, F4, and U3 within WCA-2A (in October 2009, April 2010, August 2011, and January, August, and December 2012) and site W3 within WCA-3A (in February 2012 and March and April 2013). Soil cores were sectioned to an interval of 2 cm or 4 cm from the top after removing floc to minimize inclusion of the major O_2 interface regions. A portion of each soil sample (approximately 50 to 100 g) was immediately frozen on dry ice and transported to the laboratory in Gainesville, FL, where the soils were stored at −80°C until the isolation of nucleic acids or geochemical analysis. The remaining soils were used for incubation studies within 1 week. In addition, 5 to 10 liters of surface water was collected from each site in 10-liter polypropylene bottles, which served as the source water for incubation studies. Pore water samples were collected from each sampling location and stored as described by Holmes et al. (14).

Nucleic acid isolation, PCR, clone library construction, and sequence analyses. DNA was isolated from 0.2 g (wet weight) of soil using PowerSoil DNA isolation kits (MO BIO Laboratories, Carlsbad, CA). Total RNA was isolated from 2.0 g of soil using a MO BIO PowerSoil total RNA isolation kit. The residual DNA in the RNA extracts was removed using a MO BIO RTS DNase kit. RNA was converted to cDNA using SuperScript III first-strand synthesis SuperMix including random hexamers as reverse transcriptase PCR primers (Invitrogen, Carlsbad, CA). Nucleic acids were stored at −80°C until use.

Clone libraries were constructed for analysis of the methyl coenzyme M reductase (*mcrA*) gene and the dissimilatory (bi)sulfite reductase (*dsrB*) gene. The *mcrA* gene in soil DNAs from sites F1, F4, and U3 (sampled in October 2009; depth, 0 to 2 cm) was amplified using primers mlas/mcrA-rev as previously described by Steinberg and Regan (30). Reverse transcription-PCR (RT-PCR) was performed to amplify *dsrB* from cDNA derived from F4 soils (August 2012; depth, 0 to 4 cm) using primers DSRp2060F/DSR4R as described by Foti et al. (31). The PCR products were cloned and subsequently transformed into *Escherichia coli* TOP10 by use of a TOPO TA cloning kit for sequencing (Invitrogen, Carlsbad, CA). The transformants were randomly selected on Luria-Bertani (LB) agar plates containing kanamycin (50 $\mu g \cdot ml^{-1}$) and sent to the University of Florida Sequencing Core Laboratory (http://www.biotech.ufl.edu/) for sequencing of the inserts.

All DNA sequences determined in this study were converted *in silico* into the corresponding amino acid sequences by use of the BioEdit (v.7.1.3) program (32). For phylogenetic analysis, reference sequences of *mcrA* or *dsrB* with a high similarity to the sequences recovered in the present study on a BLAST search against the sequences in the NCBI database (http://www.ncbi.nlm.nih.gov/) were collected. Reference sequences of a variety of taxa were also obtained on the FunGene website (http://fungene.cme.msu.edu/), and environmental sequences were obtained from previously published literature. Selected sequences representing operational taxonomic units (OTUs) with 5% differences in amino acid sequences were pooled with the reference sequences and aligned by use of the ClustalX (v.2.0) program (33). The alignment was used as the input file for phylogenetic analysis in MEGA (v.5.2) software (34). The phylogenetic tree was constructed using the maximum likelihood method with bootstrap analysis (1,000 resamplings).

The deduced amino acid sequences were assigned to OTUs on the basis of the percent differences between the sequences (e.g., 1%, 5%, 10%) using the furthest-neighbor method in the program mothur (v.1.31.2) (35). The mothur program was also used to estimate the diversity of OTUs and the coverage of OTUs sampled within each clone library and to create a Venn diagram showing the number of OTUs shared between clone libraries. Fast UniFrac online analysis (36) was performed for principal coordinates analysis (PCoA), phylogenetic test (37), UniFrac significance test (38), and hierarchical cluster analysis (38).

(RT-)qPCR for *mcrA*. The numbers of *mcrA* copies were estimated using quantitative PCR (qPCR) with the universal primer set targeting total methanogens (T-M), mlas/mcrA-rev (39). Three forward primers, primers MM-F (5′-CAA GTW YGG MGG ATT CGC CAA GG-3′), MST-F (5′-CAA GTW YGG MGG ATT CGC CAA GG-3′), and MB-F (5′-AAG CAC CWA ACA MCA TGG AHA CHG T-3′), were designed to enumerate the organisms in the groups *Methanomicrobiales*, *Methanosaetaceae*, and *Methanobacteriales*, respectively. The conserved sequence region for each group was used for primer design (see Fig. S2 in the supplemental material). These forward primers made a pair with the universal primer mcrA-rev in PCRs (see Table S1 in the supplemental material). The specificity of the primers was verified by analysis of sequences amplified by the group-specific primers. A total of 21, 28, and 26 clones were randomly selected from clone libraries constructed from PCR products using the primers MM-F, MST-F, and MB-F combined with mcrA-rev, respectively. All sequences from selected clones were matched to the target groups.

All qPCRs were conducted using iQ SYBR green supermix (Bio-Rad Laboratories, Hercules, CA) in a StepOnePlus real-time PCR system (Applied Biosystems, Foster City, CA). The reaction mixture contained 10 μl of iQ SYBR green supermix, 2 μl of primers (concentration of each primer, 10 $pmol \cdot \mu l^{-1}$), and 2 μl of DNA (cDNA for RT-qPCR) in a 20-μl final volume. qPCR cycling parameters were 3.5 min at 95°C, followed by 6 cycles of touchdown PCR (30 s at 95°C, 45 s with a 1°C-per-cycle decrement from 60°C to the final annealing temperature, 30 s at 72°C) and 34 cycles of the main PCR (denaturation at 95°C for 30s, annealing at 55°C for 45 s, and extension at 72°C for 30 s, image capture at 80°C for 15 s, and a final extension at 72°C for 7 min). All qPCR runs included an image capture step (15 s at 80°C) after the final extension step of each cycle and a melt curve analysis (in which the temperature was increased from 60 to 95°C in 0.5°C increments every 10 s) when the PCR amplification was completed.

Copy numbers of *dsrB* were estimated using primers DSRp2060F/DSR4 under the cycling conditions described by Foti et al. (31). The reaction mixture was prepared as described above for the *mcrA* qPCR, except that *dsrB*-specific primers were used.

For all (RT-)qPCRs, (c)DNA from each soil sample was applied in triplicate to a 96-well PCR plate with a 10-fold dilution series of a plasmid

carrying the gene fragment of interest (plasmid DNA standard). The plasmid DNA standard was prepared by cloning the target gene fragment amplified from soil samples using the same primer set used for qPCR. The insertion of the correct gene fragments of the plasmid DNA standard was confirmed by sequence analysis. The prepared plasmid DNA standards were stored in aliquots at −80°C, and a separate standard was used for each qPCR run. The PCR efficiency (E) was calculated using the formula $-1 + 10^{(-1/\text{slope})}$. The PCR efficiency measured using plasmid DNA standards under the above-described conditions for *mcrA* and *dsrB* ranged from 93.4 to 96.7% (see Table S2 in the supplemental material).

Soil incubation experiments. Several soil incubation experiments were conducted to measure methane production rates, sulfate reduction rates, and the isotopic compositions of CH_4 and CO_2. Each treatment was conducted in triplicate. All incubations were performed at 28°C in the dark. Bottles were shaken by inversion a few times every 1 or 2 days (for determination of the CH_4 production rate) or on a shaking incubator at 125 rpm (for determination of the SO_4^{2-} reduction rate).

(i) CH_4 production rate. Ten grams of surface soil (depth, 0 to 4 cm) was mixed with 10 ml of site water in triplicate 60-ml serum bottles closed with rubber stoppers and aluminum seals. The headspace gas of the bottles was exchanged by flushing N_2 through syringe needles for 10 min. The bottles were supplemented with 4 mM acetate or an H_2-CO_2 mixture (80%-20%, vol/vol) to 50 kPa. Bottles with no substrate addition were used as controls. The CH_4 concentration was analyzed on days 3, 7, and 14, as described below.

(ii) SO_4^{2-} reduction rate. Sulfate reduction rates were measured according to previously described methods (40, 41) with a slight modification as described by Castro et al. (42). Sulfate reduction rates were calculated as described by Fossing and Jørgensen (43).

(iii) Isotope composition of CH_4 and CO_2. Ten grams of soil was incubated with 10 ml of surface water in 60-ml serum bottles closed with a rubber stopper and an aluminum seal. MoO_4^{2-} (20 mM) was added to half of the incubation vials. Headspace gas was taken on incubation days 5, 8, and 12 to measure the CH_4 production rates. The stable isotopes of CH_4 and CO_2 were determined as described below. The headspace of vials containing samples from sites F1 and U3 was sampled on day 12. The headspace of vials containing samples from site F4 was sampled on day 27 because there was not enough CH_4 in the headspace for isotopic measurement until then.

(iv) Potential SAO activity. Potential syntrophic acetate-oxidizing (SAO) activity was measured as described by Hori et al. (44). Briefly, 5 g of soil was anaerobically incubated with 15 ml of surface water in 60-ml serum bottles with acetate labeled with ^{13}C at either the C_1 or C_2 position or both the C_1 and C_2 positions (Sigma Biochemicals) to a final concentration of 0.5 mM in separate incubations. After 6 days of incubation (12 days for site U3 soils), the concentrations of $^{12}CH_4$ and $^{13}CH_4$ in the headspace gases were analyzed as described below. Briefly, this method is based on the fact that the syntrophic acetate oxidation and acetoclastic pathways yield methane from carbons at different positions in the acetate molecule.

Analytical methods. Total phosphorus (TP), total carbon (TC), and total nitrogen (TN) concentrations were determined according to methods described by White and Reddy (45).

The CH_4 concentrations in soil incubation and pore waters were measured from the headspace using a Shimadzu 8A gas chromatograph equipped with a Carboxen 1000 column (Supelco, Bellefonte, PA) and a flame ionization detector operating at 110°C as described previously (10). The CH_4 concentration in the aquatic phase was calculated using Henry's law constant for CH_4 (1.3×10^{-3} mol · liter^{-1} · atm^{-1} at 298 K) (46; http://henrys-law.org).

The H_2 concentrations in pore waters were measured from the headspace of the bottles using a Peak Performer 1 gas analyzer (Peak Laboratories, Mountain View, CA) with a reducing compound photometer. The H_2 concentration in the aquatic phase was calculated using Henry's law constant for H_2 (7.8×10^{-4} mol · liter^{-1} · atm^{-1} at 298 K) (46).

Acetate was derivatized with 2-nitrophenyl hydrazide, and the derivative was separated by use of a high-pressure liquid chromatography system (Waters 2695; Waters Corp., Milford, MA) equipped with a Platinum EPS C_8 column (1.6 by 250 mm; Alltech, Deerfield, IL) under a gradient profile composed of two mobile phases, as described by Albert and Martens (47). The derivative was detected at 400 nm with a UV absorbance detector (Waters 2487; Waters Corp.).

The composition of $\delta^{13}CH_4$ and $\delta^{13}CO_2$ in the headspace of the incubation bottles was determined using a Finnigan Mat Delta V isotope ratio mass spectrometer coupled to a gas chromatograph, as described by Merritt et al. (48).

Statistical analyses. The significances in the differences in gene copies, microbial activities, and chemical data between study sites or treatments were computed using one-way analysis of variance (ANOVA) or Student's t test with JMP (v.10) software (SAS Institute Inc., Cary, NC, USA), followed by the *post hoc* Tukey-Kramer honestly significant difference (HSD) test for ANOVA. P values of <0.05 were considered significant. For exploring the relationships between variations in gene copy numbers and geochemical parameters, a redundancy analysis (RDA) was implemented in Canoco (v.4.5 for Windows) software (49). The statistical significances of axis and individual parameters were evaluated using a Monte Carlo permutation full model with 999 unrestricted permutations.

Nucleotide sequence accession numbers. The GenBank accession numbers for the sequences determined in this study are KR075171 to KR075423 for *mcrA* and KR075424 to KR075502 for *dsrB* transcript sequences.

RESULTS

Site descriptions and biogeochemical characteristics. Sites F1, F4, and U3 are located within WCA-2A of the northern Everglades (see Fig. S1 in the supplemental material), where agricultural drainage from EAA has resulted in a north-to-south gradient in soil P concentrations (50). The soil P concentrations in the samples used for this study were 1.28 g · kg^{-1} in site F1, the northernmost site; 0.59 g · kg^{-1} in site F4; and 0.25 g · kg^{-1} in site U3, the southernmost site (Table 1). These values are in good agreement with previously reported results (42, 51). In contrast to the soil P concentration gradient, a sharp gradient in SO_4^{2-} concentrations was not observed in surface waters (176 to 200 μM) or soil pore waters (39 to 56 μM) (52). Acetate and H_2 concentrations were highly variable, and average values are presented in Table 1. No significant differences were observed between the sites due to the high variability among the samples.

Site W3 is located in the interior region of WCA-3A (see Fig. S1 in the supplemental material), such that it is removed from the direct influence of surface water discharges. The site harbors relatively low soil P concentrations (0.38 g · kg^{-1}), similar to site U3 in WCA-2A; however, this site is distinguished from the WCA-2A sites by a much lower SO_4^{2-} concentration (≤4 μM) in surface waters and pore waters (52). Site W3 is therefore valuable for comparison with the WCA-2A sites. The sites selected for this study are distinct from each other with respect to the concentrations of soil P and surface water SO_4^{2-}: site F1 has high P and high SO_4^{2-} concentrations, site F4 has an intermediate P concentration and a high SO_4^{2-} concentration, site U3 has a low P concentration and a high SO_4^{2-} concentration, and site W3 has low P and SO_4^{2-} concentrations.

Diversity and distribution of McrA sequences. A total of 255 *mcrA* sequences were obtained from three clone libraries derived from site F1, F4, and U3 soils in WCA-2A and were translated *in silico* to amino acid sequences (henceforth referred to as McrA

TABLE 1 Summary of geochemical characteristics of soils and pore waters and rates of CH_4 production and SO_4^{2-} reduction measured in WCA soils[a]

Site	Coordinates	Soil chemistry[b]			Pore water chemistry[c]			CH_4 production rate (μmol · g $soil^{-1}$ · day^{-1})[e]			SO_4^{2-} reduction rate (μmol · g $soil^{-1}$ · day^{-1})[e]		
		TP concn (g/kg)	TN concn (g/kg)	TC concn (g/kg)	Acetate concn (μM)	H_2 concn (μM)	SO_4^{2-} concn (μM)[d]	Intact soils	Acetate	H_2-CO_2	Intact soils	Acetate	H_2-CO_2
F1	26°21′39″N, 80°22′10″W	1.28 ± 0.24	31 ± 3	442 ± 31	19.5 ± 9.9	0.33 ± 0.10	56 ± 86	3.1 ± 3.2	5.3 ± 1.4	11.6 ± 3.5	0.5 ± 0.4	1.4 ± 0.3	1.2 ± 1.0
F4	26°18′59″N, 80°23′01″W	0.59 ± 0.26	34 ± 3	424 ± 29	25.9 ± 33.8	0.28 ± 0.20	74 ± 110	0.9 ± 0.9	2.7 ± 0.5	5.6 ± 2.9	<0.01	0.1 ± 0.1	<0.01
U3	26°17′15″N, 80°24′41″W	0.25 ± 0.04	27 ± 5	385 ± 69	17.1 ± 16.4	0.28 ± 0.14	39 ± 35	<0.1	0.4 ± 1.2	2.1 ± 1.0	0.03 ± 0.04	0.07 ± 0.07	0.14 ± 0.17
W3	26°02′35″N, 80°49′39″W	0.38 ± 0.02	36 ± 1	424 ± 4	ND[f]	ND	≤4	ND	ND	ND	ND	ND	ND

[a] Data represent means ± SDs.
[b] Soil chemistry in topsoils (0 to 4 cm) sampled in April 2010 and August and December 2012 from the WCA-2A sites ($n = 9$ from triplicates of each sample) and April 2013 from site W3 ($n = 6$) was assayed.
[c] Acetate and H_2 concentrations were measured in pore waters (0 to 4 cm) sampled in April 2010 and August 2011 ($n = 6$).
[d] SO_4^{2-} concentrations for sites F1, U3, and W3 were adapted from our previous study (52), with additional data for samples from site F4 collected in April 2010 and August and December 2012 ($n = 9$) being analyzed in this study.
[e] The rates of methane production and SO_4^{2-} reduction were measured in incubations with soils (depth, 0 to 4 cm) sampled in August 2012. Acetate (4 mM) and H_2-CO_2 (50 kPa) were added in triplicate.
[f] ND, not determined.

sequences) for further analysis. The McrA sequences were grouped into 96 OTUs defined by a 5% difference in amino acid sequences. The Chao1 richness estimator predicted the presence of 58 to 74 OTUs, with the highest number being observed for the sequences from site F1. The Shannon diversity indices (range, 3.4 to 3.6) did not differ significantly between sites. Coverage statistics indicated that 71 to 78% of the OTUs in each library were accounted for in this study (see Table S3 in the supplemental material).

The 96 OTUs were distributed within the orders *Methanomicrobiales*, *Methanosarcinales*, *Methanocellales*, *Methanobacteriales*, and *Methanomassiliicoccales*. The isolate of the *Methanomassiliicoccales* is related to recently isolated *Methanomassiliicoccus luminyensis* B10 (53) and to "*Candidatus* Methanomethylophilus alvus" Mx1201 retrieved from genomes derived from a human gut (54) (Fig. 1). Detailed phylogenetic affiliations for the OTUs are provided in Table S4 in the supplemental material.

One hundred forty-four sequences (accounting for 56% of all sequences) made up 50 OTUs belonging to the order *Methanomicrobiales*. Of the OTUs belonging to the *Methanomicrobiales*, 24 OTUs clustered within the family *Methanomicrobiaceae* (*Methanomicrobiales* subclades I [9 OTUs] and II [15 OTUs]), and 13 OTUs clustered within the *Methanoregulaceae* (*Methanomicrobiales* subclades V [6 OTUs] and VII [7 OTUs]). The remaining 13 OTUs were divided into novel *Methanomicrobiales* clades III (2 OTUs), IV (7 OTUs), and VI (4 OTUs), which did not include previously taxonomically defined methanogens. Sixty sequences (accounting for 25% of all sequences) made up 24 OTUs belonging to the order *Methanosarcinales*; of these, 22 OTUs were assigned to the *Methanosaetaceae* and 2 OTUs were assigned to the *Methanosarcinaceae*. Twenty sequences (7.8% of all sequences) made up eight OTUs belonging to the order *Methanobacteriales*, and *Methanobacteriales* were present as a minor group (≤10.4%) at all sites. One *mrtA* sequence (*Methanobacteriales* clade I) which is usually detected in *Methanobacteriales* as an isozyme of McrA (55) was found in the library of sequences from site F1. Four OTUs belonging to the *Methanomasiliicoccales* were included as a minority (≤5.7%) in the libraries of clones from sites F1 and U3, but no sequence belonging to the *Methanomasiliicoccales* was found at site F4. Nine OTUs belonging to the *Methanomasiliicoccales* group were included in the libraries of clones from sites F1 (accounting for 6.9% of all site F1 sequences) and U3 (14.9% of all site U3 sequences), and this group was further divided into subgroups I and II, with subgroup II including strains B10 and Mx1201.

The differences in the McrA assemblages between sites F1, F4, and U3 were clearly illustrated by the compositions and relative abundances (in percent) of subclades for each site, as depicted in the stacked-column graph on the right in Fig. 1. Of 96 OTUs, only 4 OTUs were shared between the three sites, and less than 15 OTUs were shared between two sites (see the Venn diagram in Fig. S3 in the supplemental material). Significant differences between assemblages were statistically verified ($P \leq 0.001$) by the phylogenetic test (37) and UniFrac significance test (38) in the UniFrac implementation. In a scatter plot of an unweighted PCoA, all assemblages were clearly separated by either principal component 1 (explaining 62.57% of the variation) or principal component 2 (explaining 37.43% of the variation), which is in good agreement with the largely separate assemblages represented in a hierarchical tree (see Fig. S3 in the supplemental material).

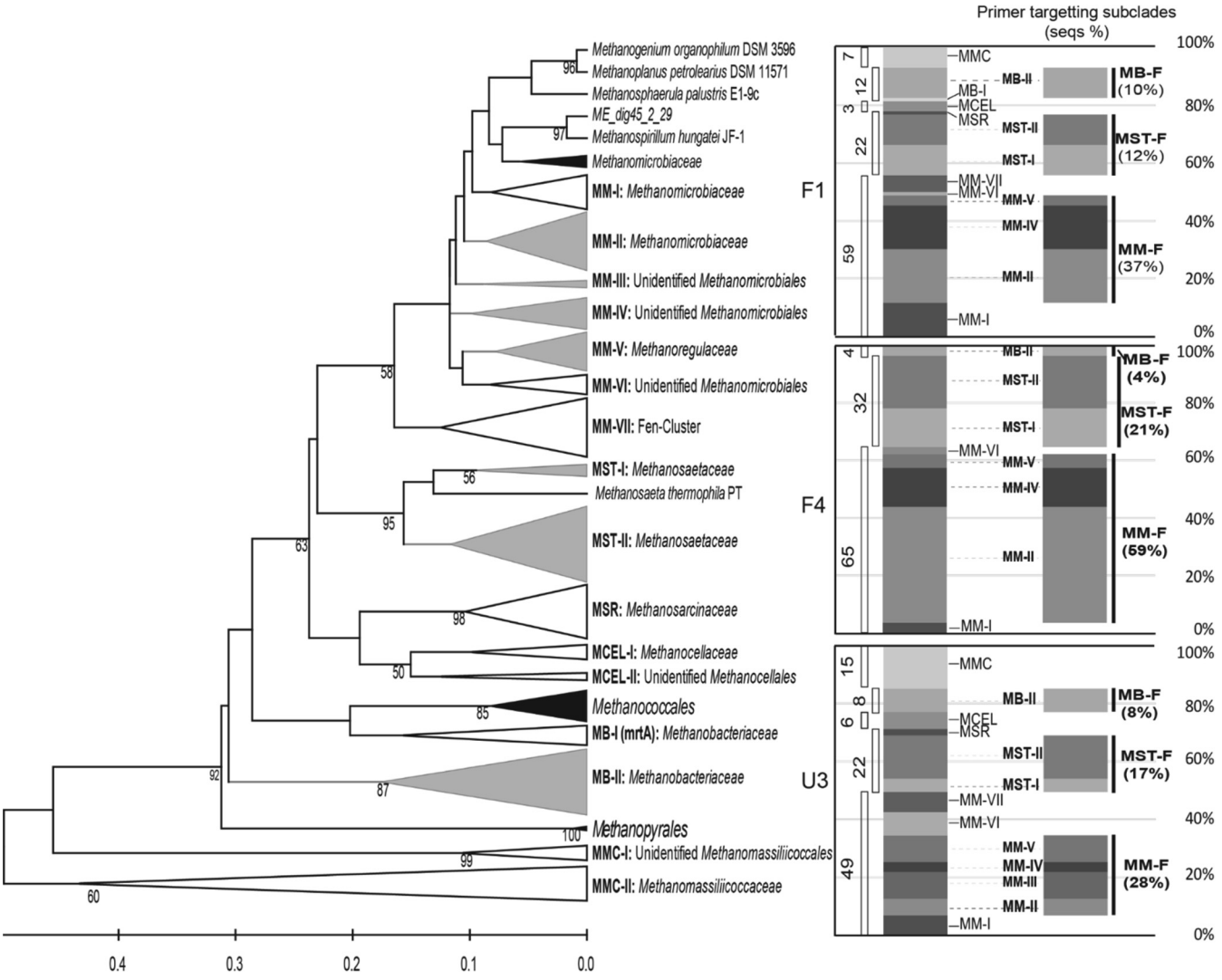

FIG 1 (Left) Maximum likelihood tree representing the phylogeny of amino acid sequences (seqs) deduced from the sequences of *mcrA* genes retrieved from soils taken from sites F1, F4, and U3 in October 2009. Bootstrap values of ≥50% from 1,000 reassemblages are placed at the branch points. Gray, clades targeted by the group-specific primers designed in the present study; white, clades containing only sequences from this study; black, clades with reference sequences and not containing sequences from this study. (Right) Relative percentages of clades generated from the maximum likelihood tree and the clades targeted by the currently designed primers. MMC, *Methanomasiliicoccales*; MB, *Methanobacteriales*; MCEL, *Methanocellales*; MSR, *Methanosarcinaceae*; MM, *Methanomicrobiales*; MST, *Methanosaetaceae*.

qPCR enumeration of *mcrA* and *dsrB* copies. (i) *mcrA* copy numbers. The numbers of *mcrA* copies were estimated for total methanogens and for the groups *Methanomicrobiales*, *Methanosaetaceae*, and *Methanobacteriales*. Since the *mcrA* sequences from WCA-2A were largely unique and diverse, new primers MM-F, MST-F, and MB-F were designed to enumerate these groups. Degenerative primer MM-F targets the major groups of the *Methanomicrobiales* included in subclades II, III, IV, and V, which included 73% of the WCA-2A *Methanomicrobiales* sequences (Fig. 1). Primer MST-F targets *Methanosaetaceae* sequences on branches that include 70% of the WCA-2A *Methanosaetaceae* sequences, with the exception of one branch closely related to *Methanosaeta harundinacea*. Primer MB-F targets the *Methanobacteriales*, and its sequence was highly matched to all the WCA-2A *Methanobacteriales* sequences. Even though there was some variation among the sites, the relative proportions of sequences targeted by primers MM-F, MST-F, and MB-F were consistent with the proportions of *Methanomicrobiales*, *Methanosaetaceae*, and *Methanobacteriales* in the order *Methanomicrobiales* > *Methanosaetaceae* > *Methanobacteriales* for each clone library (Fig. 1). Therefore, qPCR using these primers is believed to be appropriate for estimating the relative number of target groups within and between sites.

qPCR for *mcrA* in soil samples collected in different seasons from 2009 to 2013 was conducted (see Table S5 in the supplemental material). Three subsamples were taken at each time point, and then the amounts were averaged for analysis. A one-way ANOVA blocked by time was run for each of the sites and for the different response variables. When significant differences in the numbers of genes were found, the Tukey-Kramer HSD test was used determine which genes differed in number (see Fig. S4 in the supplemental material).

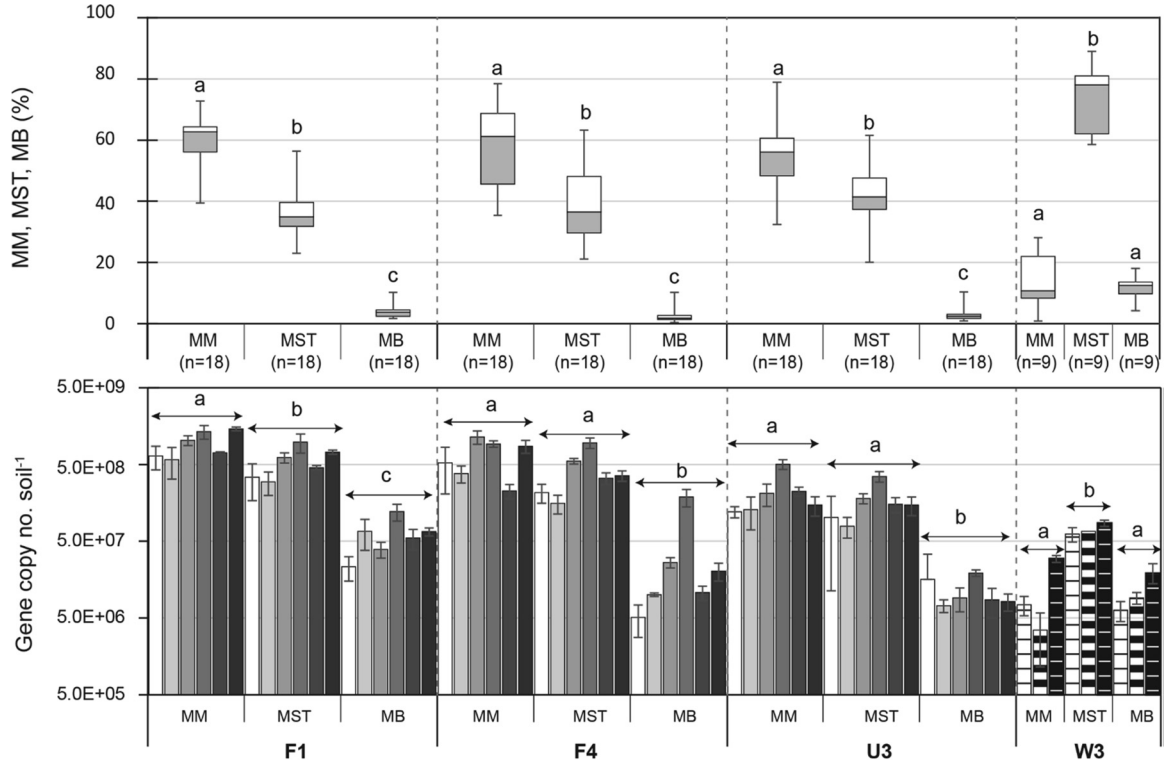

FIG 2 Box-and-whisker plot (top) and temporal profile (bottom) of the copy numbers of *mcrA* from *Methanomicrobiales*, *Methanosaeta* (*Methanosaetaceae*), and *Methanomicrobacteriaceae* (*Methanobacteriales*) in WCA soils. Data in the temporal profile are presented in order of sampling: from the left, October 2009, April 2010, August 2011, and January, August, and December 2012 for WCA-2A sites F1, F4, and U3 and February 2012 and March and April 2013 for site W3. Error bars in the bar graph represent ±1 SE ($n = 3$). Box-and-whisker plots were generated from the pooled data from the temporal profile. Boxes depict the medians (horizontal lines in the boxes) and the lower and upper quartiles (bottoms and tops of the boxes, respectively). The vertical bars (whiskers) show the highest and the lowest values, excluding outliers. The different letters indicate a significant difference among the groups *Methanomicrobiales*, *Methanosaetaceae*, and *Methanobacteriales* ($P < 0.05$ by the Tukey-Kramer HSD test).

qPCR for the groups *Methanomicrobiales*, *Methanosaetaceae*, and *Methanobacteriales* revealed that the *Methanomicrobiales* and/or *Methanosaetaceae* were dominant in all WCA sites; however, the *Methanomicrobiales* were dominant in WCA-2A and the *Methanosaetaceae* were dominant in WCA-3A. Within all WCA-2A sites, the *Methanomicrobiales mcrA* copy numbers (2.2 to 9.6 × $10^8 \cdot$ g soil^{-1}, on average) were higher than the *Methanosaetaceae mcrA* copy numbers (1.7 to 5.7 × $10^8 \cdot$ g soil^{-1}, on average) (Fig. 2; see also Table S5 in the supplemental material). A one-way ANOVA blocked by time revealed that the *Methanomicrobiales mcrA* copy numbers were higher than the *Methanosaetaceae mcrA* copy numbers in site F1 ($P < 0.05$) but were not significantly different from the numbers in the other sites, due to the temporal variation within each site (Fig. 2, bottom). Comparison of the percentages of each group within individual samples ([number of *mcrA* copies for one group]/[total numbers of *mcrA* copies for the *Methanomicrobiales*, *Methanosaetaceae*, and *Methanobacteriales* combined] × 100) more clearly showed that the percentage of *Methanomicrobiales* was significantly higher than the percentage of *Methanosaetaceae* (Tukey-Kramer HSD test, $P < 0.0001$) in all the WCA-2A sites (Fig. 2). In contrast, for site W3 it was found that the *Methanosaetaceae* significantly outnumbered the *Methanomicrobiales* according to both the absolute number of *mcrA* copies (7.8 × $10^7 \cdot$ g soil^{-1} versus 1.9 × $10^7 \cdot$ g soil^{-1}, on average) and the relative percentage of *mcrA* copies (73.9% ± 11.6% versus 14.2% ± 9.0% [mean ± standard deviation {SD}]) ($P < 0.0001$ for both comparisons).

(ii) *dsrB* copy numbers. The number of *dsrB* copies estimated in WCA soils ranged from 5.1 × 10^7 to 4.9 × $10^9 \cdot$ g soil^{-1} (see Fig. S5 and Table S5 in the supplemental material). WCA-2A sites showed significant variations in *dsrB* copy numbers by season (one-way ANOVA, $P < 0.001$ within each site), while site W3 in WCA-3A did not (one-way ANOVA, $P = 0.8855$) (see Fig. S5 in the supplemental material). In all WCA-2A sites, the highest *dsrB* copy numbers were obtained in January, while the lowest copy numbers were observed in April. Comparison of the pooled temporal data from each site indicated that the *dsrB* copy numbers were significantly different among the sites (one-way ANOVA, $P < 0.001$) (see Fig. S5 in the supplemental material). Site F1 had the highest number (1.88 × $10^9 \cdot$ g soil^{-1}, on average), followed by sites F4 (1.52 × $10^9 \cdot$ g soil^{-1}), U3 (6.72 × $10^8 \cdot$ g soil^{-1}), and W3 (8.55 × $10^7 \cdot$ g soil^{-1}), in that order.

The *dsrB* copy numbers were significantly higher than the T-M *mcrA* copy numbers in the WCA-2A sites (Student's *t* test, $P < 0.05$) but were not significantly different from the copy numbers in site W3 (Student's *t* test, $P = 0.86$) (Fig. 3).

Relatedness of *mcrA* and *dsrB* copy numbers to geochemical parameters. Redundancy analysis (RDA) was performed to evaluate the relationships between the abundances of methanogens and SRPs and the geochemical concentrations in the WCAs. T-M

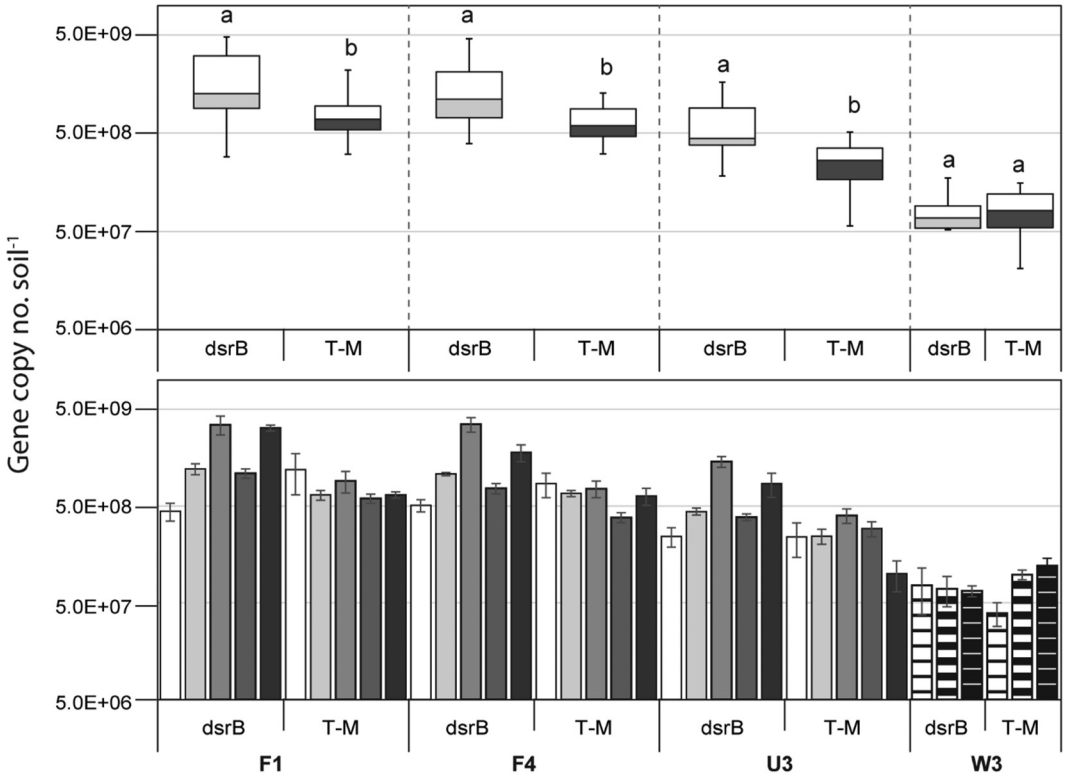

FIG 3 Box-and-whisker plot (top) and temporal profile (bottom) of the *dsrB* copy numbers compared with the T-M *mcrA* copy numbers estimated in the same sample. Data in the temporal profile are presented in order of sampling: from the left, April 2010, August 2011, and January, August, and December 2012 for WCA-2A sites F1, F4, and U3 and February 2012 and March and April 2013 for site W3. Error bars in the bar graph represent ±1 SE ($n = 3$). The box-and-whisker plot was constructed from the pooled data from the temporal profile. Boxes depict the medians (horizontal lines in the boxes) and the lower and upper quartiles (bottoms and tops of the boxes, respectively), while the whiskers show the highest and the lowest values, excluding outliers. The different letters indicate a significant difference between *dsrB* and T-M *mcrA* copy numbers ($P < 0.05$ by Student's *t* test).

copy numbers were positively correlated with TP concentrations (Fig. 4). *dsrB* copy numbers were also positively correlated with SO_4^{2-} and TP concentrations. The positive correlations of T-M and *dsrB* copy numbers with those geochemical parameters were due to the elevated numbers in the presence of higher P and SO_4^{2-} concentrations by site in the order F1 > F4 > U3 > W3, as described above.

RDA was also applied to the relative proportions of *Methanomicrobiales*, *Methanosaetaceae*, and *Methanobacteriales* within each sample to observe the relationships between the compositions of these methanogenic groups and geochemical factors. The percentage of *Methanomicrobiales* was positively correlated with TP and SO_4^{2-} concentrations, while the percentages of *Methanosaetaceae* and *Methanobacteriales* were negatively correlated with those parameters.

Levels of *mcrA* and *dsrB* gene expression. In order to assess the extent to which the genes were transcribed, RT-qPCR for *mcrA* and *dsrB* and potential activity for methanogenesis and sulfate reduction (to indirectly measure the levels of enzymes encoded by the corresponding genes) were determined in the samples from the WCA-2A sites collected in August 2012. The average *mcrA* mRNA copy numbers were as follows: $1.7 \times 10^7 \cdot$ g soil^{-1} in site F1, 1.1×10^6 in site F4, and $9.3 \times 10^4 \cdot$ g soil^{-1} in site U3. The average *dsrB* mRNA copy numbers were 1.6×10^6 in site F1, $9.0 \times 10^4 \cdot$ g soil^{-1} in site F4, and $5.9 \times 10^4 \cdot$ g soil^{-1} in site U3. The mRNA copy numbers were 2 to 4 orders of magnitude lower than the gene copy numbers; however, they followed the order of the gene copy numbers according to the SO_4^{2-} and P gradient, i.e., F1 > F4 > U3 (Fig. 5). Likewise, the numbers of copies of cDNA from the *Methanomicrobiales*, *Methanosaetaceae*, and *Methanobacteriales* were consistent with the relative abundances of the gene copy numbers within sites and among the sites.

Potential methane production rates were 3.1 μmol · g soil^{-1} · day^{-1} in site F1 soils, 0.9 μmol · g soil^{-1} · day^{-1} in site F4 soils, and less than 0.1 μmol · g soil^{-1} · day^{-1} in site U3 soils (Table 1). Potential SO_4^{2-} reduction rates were 0.5 μmol · g soil^{-1} · day^{-1} in F1 soils, which were higher than those measured in F4 and U3 soils (≤0.03 μmol · g soil^{-1} · day^{-1}). These potential activities for CH_4 production and SO_4^{2-} reduction were in good agreement with the order of the levels of the *mcrA* and *dsrB* copy numbers measured along nutrient gradients (F1 > F4 > U3); hence, the gene copy numbers measured throughout this study are likely to predict the level of gene expression in each site.

Impact of SRP activities on methanogenesis. Soil incubation studies were conducted to evaluate the potential influence of SRP activities on methanogenic pathways and, correspondingly, on the shaping of the methanogen assemblage structure. The incubation was done using the WCA-2A soils with relatively high SO_4^{2-} concentrations in the presence or absence of MoO_4^{2-}, a specific inhibitor of SRP activity. Soil incubation studies showed higher methane production rates in soils treated with MoO_4^{2-} (a specific inhibitor of SRP activity) for all sites (Fig. 6A): 1.9 · g soil^{-1} · day^{-1}

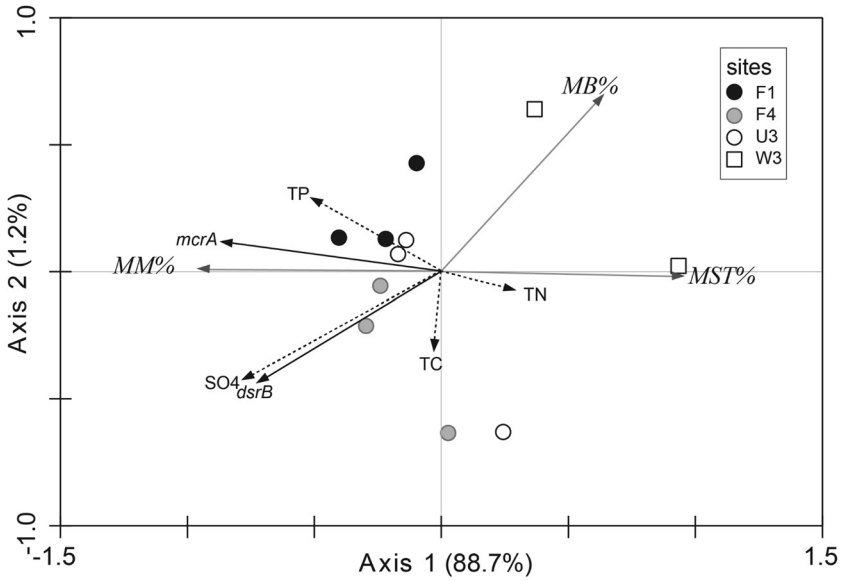

FIG 4 Results of RDA presenting the correlation between *mcrA* and *dsrB* copy numbers and geochemical parameters obtained for the samples from sites F1, F4, and U3 collected in April 2010 and August and December 2012 and the samples from site W3 collected in February 2012 and April 2013. Arrows pointing in the same direction indicate positive correlations, and arrows pointing in opposite directions indicate negative correlations. The arrow length corresponds to the variance explained by the environmental variable. The first two axes explain 89.9% of the total canonical eigenvalues with a significant Monte-Carlo test value ($P < 0.05$).

for treated soils versus 1.3 μmol · g soil^{-1} · day^{-1} for untreated soils in site F1, 1.3 versus 0.6 μmol · g soil^{-1} · day^{-1} in site F4, and 0.5 versus 0.05 μmol · g soil^{-1} · day^{-1} in site U3 (Fig. 6A). These findings indicate that methanogens and SRPs are in competition for common substrates.

MoO_4^{2-} treatment resulted in increases in the levels of $\delta^{13}CH_4$: −67‰ to −55‰ in site F1 and −76‰ to −57‰ in site F4. The small amount of CH_4 produced in U3 soil incubations without added MoO_4^{2} prohibited measurement of $\delta^{13}C$, but in incubations with Mo treatment, the level of $\delta^{13}CH_4$ was −57‰ in site U3 (Table 2; Fig. 6B). In contrast, there was no significant difference in the amount of $\delta^{13}CO_2$ observed between the control soils and the MoO_4^{2-}-treated soils. The apparent fractionation factor (α_{app}) quantifies the isotopic difference between CH_4 and CO_2 and is a generally accepted index used to estimate the contribution of a particular methane production pathway to a methane pool (56, 57). MoO_4^{2-} treatment reduced α_{app} from 1.054 to 1.040 in site F1 and 1.060 to 1.041 in site F4, indicating a shift toward the acetoclastic pathway.

Inhibition of SRP activity using MoO_4^{2-} resulted in an increase in the relative *mcrA* transcript level for the *Methanosaetaceae* from 27 to 43% in site F1 soils and from 48% to 55% in site F4 soils (Fig. 7), consequently reducing the relative percentage of *Methanomicrobiales mcrA* transcripts. With MoO_4^{2-} treatment, the *Methanobacteriales* increased in relative percentage, from 3 to 9% in F1 soils and from 1 to 2% in F4 soils, even though this group still appeared to be a minor group. The changes in the *mcrA* transcript level in U3 soil incubations were not accurately determined due to the recovery of low levels of RNA from the incubated soils.

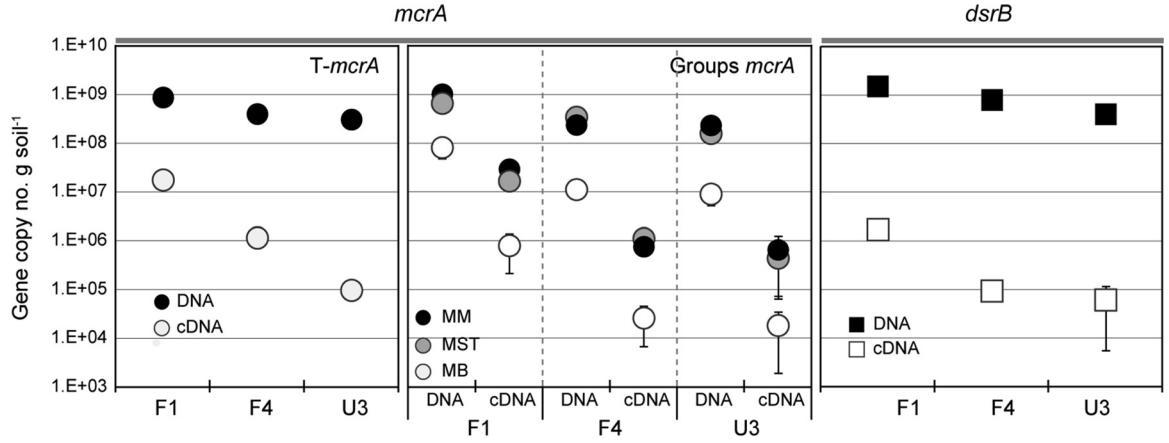

FIG 5 Numbers of copies of the *mcrA* and *dsrB* genes and their transcripts measured from surface soils (0 to 4 cm depth) sampled from WCA-2A sites F1, F4, and U3 in August 2012. Error bars represent ±1 SE ($n = 3$).

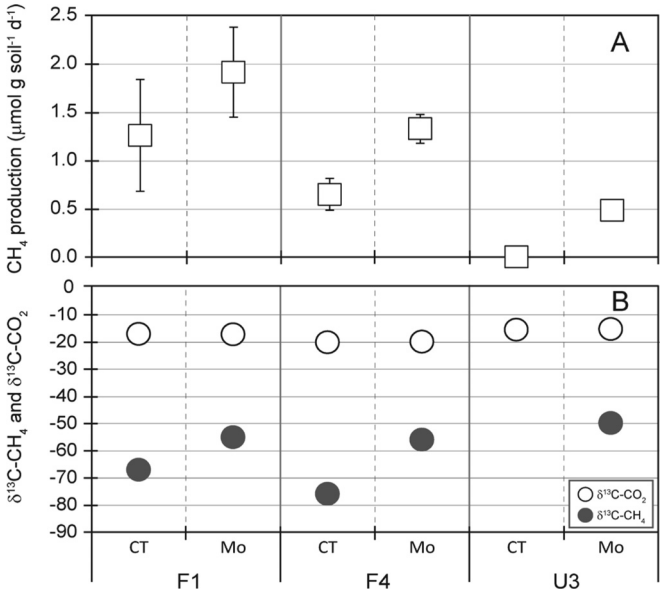

FIG 6 CH_4 production rate (A) and composition of the $\delta^{13}CH_4$ and $\delta^{13}CO_2$ produced (B) during incubation of soils sampled in August 2012. Error bars represent ±1 SD ($n = 3$; note that the control incubation of site U3 soils did not produce a detectable amount of $\delta^{13}CH_4$). CT, control without MoO_4^{2-}; Mo, addition of MoO_4^{2-} (20 mM).

DISCUSSION

The nutrient gradient in WCA-2A soils provides an excellent opportunity to study the impacts of nutrient additions to naturally P-poor wetlands. A very large body of work has been published on changes that the P additions have brought to the greater WCA-2A ecosystem, ranging from the distribution of endangered vertebrates to changes in biogeochemical cycling (49, 58). The present study builds on previous studies on the distribution and function of methanogenic and sulfidogenic guilds (10, 42, 51) and investigates controls on methanogenic pathways as a function of position along the nutrient gradient.

The methanogenic assemblage structure based on *mcrA* sequences revealed distinct features reflecting the nutrient status of WCA-2A. One of the key features was the numerical dominance and diversity of the hydrogenotrophic *Methanomicrobiales*. *Methanomicrobiales* sequences accounted for >49% of the total sequences retrieved from WCA-2A soils, and the phylogeny of the *Methanomicrobiales* was broadly distributed across 7 distinct clades, *Methanomicrobiales* clade I to clade VII. *Methanomicrobiales* have been shown to dominate in at least some acidic bogs or rice fields (30, 59); however, WCA *Methanomicrobiales* members are distinct from *Methanomicrobiales* sequences referred to as to the "fen cluster" (60) or the "rice cluster" (55) (Fig. 1).

Another feature is that the acetotrophic order *Methanosarcinales* was dominated by the *Methanosaetaceae* (≥95% of *Methanosarcinales* sequences). In general, the *Methanosaetaceae* exhibit a low threshold for acetate (61), and WCA-2A pore waters harbor low concentrations of acetate (<0.03 mM) (Table 1), as would be expected for a system dominated by the *Methanosaetaceae*. The low concentrations of acetate might result from SRP activities competing for acetate, thereby selecting for this type of acetotrophic methanogen in WCA-2A. Along with the *Methanomicrobiales* (49% to 65%), the *Methanosaetaceae* (22% to 32%) were a dominant methanogenic group in WCA-2A, such that these two groups play a significant role in determining the pathways of methanogenesis in WCA-2A.

Recently, Holmes and colleagues (14) reported that AM is the dominant pathway (50% to 75%) over HM (25% to 50%), based on the differences in CH_4 production rates in soils with and without incubation with methyl fluoride (an inhibitor of AM) and the $\delta^{13}CH_4$ and $\delta^{13}CO_2$ values in pore waters collected from the same sites used in this study. Those results do not appear to be consistent with our observation that the *Methanosaetaceae* were outnumbered by the *Methanomicrobiales* in all sites of WCA-2A. This paradoxical result might be explained by the higher free energy of formation in HM ($4H_2 + CO_2 \rightarrow CH_4 + 2H_2O$, for which $\Delta G^{o\prime}$ is equal to -135 kJ · mol CH_4^{-1}) than in AM ($CH_3COOH \rightarrow CH_4 + CO_2$, for which $\Delta G^{o\prime}$ is equal to -33 kJ · mol CH_4^{-1}) (62). This allows HM to produce larger amounts of biomass even if less CH_4 is produced by this pathway. We did not calculate ΔG for these reactions *in situ*, however, and there may be alternative explanations for these observations. Most hydrogenotrophs are able to grow with additional substrates (e.g., formate, methyl amines, methanol) other than H_2 and CO_2. For example, members of the numerically dominant group in WCA-2A, the *Methanomicrobiales*, utilize acetate as a carbon source, although they do not use it for methanogenesis (63).

Even though AM is the dominant methanogenic process overall in sites of WCA-2A, Holmes et al. (14) reported that HM became relatively more important at site F1, accounting for almost 50% of the total methane produced. These results are relatively consistent with the group-specific qPCR results reported here, where the *Methanomicrobiales* accounted for 60.3% of the organisms in site F1, 58.6% in site F4, and 55.0% in site U3, consequently decreasing the percentage of *Methanosaetaceae* in the order F1 (35.7%) < F4 (38.6%) < U3 (42.1%).

One of primary aims of this study was to evaluate the influence of SRP activities on the methanogenic pathways and the methanogen community as controlling forces in response to nutrient gradients within the WCAs. The qPCR results for the *Methanomicrobiales* and *Methanosaetaceae* across the SO_4^{2-} gradients provide evidence that SRP activity is likely involved in shaping methanogen assemblage structure and activity. In our long-term monitoring, WCA-2A sites representing SO_4^{2-}-rich environments consistently showed a dominance of the hydrogenotrophic *Methanomicrobiales*

TABLE 2 $\delta^{13}CH_4$ and $\delta^{13}CO_2$ concentrations and α_{app} values for incubated Everglades soils

Site	Treatment[a]	Concn (‰)[b]		α_{app}[c]
		$\delta^{13}CH_4$	$\delta^{13}CO_2$	
F1	CT	−67.00 ± 2.16	−17.02 ± 1.20	1.054
	Mo	−55.02 ± 1.17	−17.16 ± 0.84	1.040
F4	CT	−75.92 ± 1.00	−20.12 ± 0.88	1.060
	Mo	−57.35 ± 2.81	−18.92 ± 2.28	1.041
U3	CT	ND[d]	−17.46 ± 0.58	NA[e]
	Mo	−56.88 ± 1.67	−15.87±.053	1.043

[a] CT, control without MoO_4^{2-}; Mo, addition of MoO_4^{2-} (20 mM).
[b] Data represent means ± SDs ($n = 3$).
[c] α_{app} is defined as (amount of $\delta^{13}CO_2$ + 1,000)/(amount of $\delta^{13}CH_4$ + 1,000).
[d] ND, not determined.
[e] NA, not applicable.

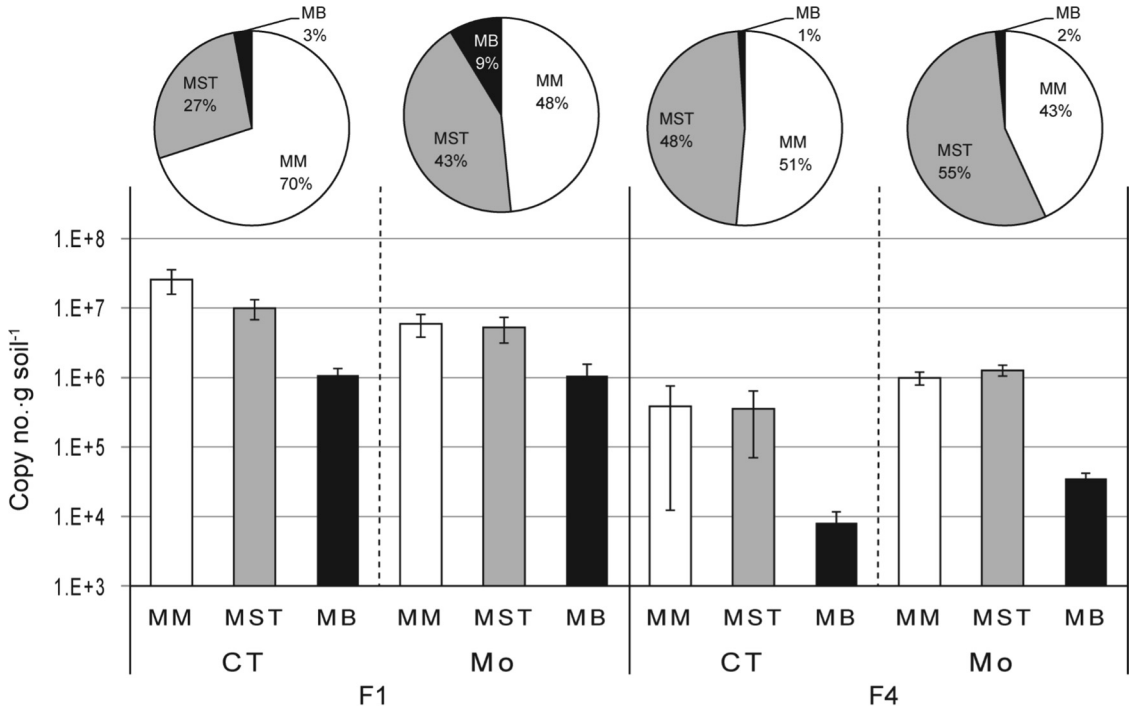

FIG 7 *mcrA* transcript copy numbers, estimated using RT-qPCR, from the incubation of soils from sites F1 and F4 sampled in August 2012. For this RT-qPCR analysis, the RNA was isolated from the soils sampled on the same date that the gas samples were collected for the $\delta^{13}CH_4$ and $\delta^{13}O_2$ analysis. CT, control without MoO_4^{2-}; Mo, addition of MoO_4^{2-} (20 mM). Error bars represent ±1 SE ($n = 3$).

(58% on average) over the acetotrophic *Methanosaetaceae* (39%), while site W3, representing a SO_4^{2-}-poor environment, revealed the opposite relationship (the *Methanomicrobiales* comprised 14% of the organisms, on average, whereas the *Methanosaetaceae* comprised 74%) (Fig. 2; see also Table S5 in the supplemental material). An RDA plot shows the positive correlation of the percentage of *Methanomicrobiales* organisms with the SO_4^{2-} concentration, while the percentage of *Methanosaetaceae* correlated negatively with the SO_4^{2-} concentration (Fig. 4). High SO_4^{2-} concentrations might cause an enrichment of sulfidogenic SRPs, which are typically thought to outcompete methanogens for acetate (26, 64), consequently decreasing the percentage of *Methanosaetaceae* while increasing the percentage of *Methanomicrobiales*.

The soil incubation study using MoO_4^{2-} as an SRP inhibitor provides evidence that SRPs control, at least to some extent, the methanogenic pathways and drive an enrichment of hydrogenotrophs, specifically, the *Methanomicrobiales* group, in WCA-2A. The addition of MoO_4^{2-} resulted in increasing values of $\delta^{13}CH_4$ and lower α_{app} values (Fig. 6B and Table 2), consistent with competition between SRPs and acetotrophic methanogens for acetate. Since the production of CH_4 by AM is generally associated with lower α_{app} values and, often, with less negative $\delta^{13}CH_4$ values than HM (56, 65, 66), those increments imply that AM was enriched by blocking SRP activity; in other words, SRP activity most likely inhibited the activities of the *Methanosaetaceae* in these soils. The increased proportion of *Methanosaetaceae mcrA* mRNA observed in the MoO_4^{2-} treatments (Fig. 7) supports this contention, which is in good agreement with the aforementioned increase in AM caused by SRP inhibition.

The specific interactions between SRP and methanogens can be quite complex. It is possible that some syntrophic fermentation of primary fermentation products, such as short-chain fatty acids or alcohols, occurred in our incubations with MoO_4^{2-}, which may have contributed to the acetate used by the *Methanosaetaceae*. Wu et al. (67) reported that MoO_4^{2-} inhibited syntrophic fermentation by SRPs to varying degrees (97% for propionate, 24% for ethanol) in a wastewater bioreactor.

An additional sink for acetate and a corresponding source of H_2 might have been via syntrophic acetate oxidation to H_2; however, we determined in separate experiments without MoO_4^{2-} that SAO was not significant in our samples (data not shown).

It should be noted that other factors, such as differences in organic carbon quality, may also impact the relative proportions of AM and HM (68). We also expected that the P concentration may be an important factor governing the methanogen composition regarding AM and HM, likely through increased primary productivity and carbon input into the soil. Increases in P concentrations correlated with increases in the population size of methanogens, such that a positive correlation between *mcrA* copy numbers and P concentrations was observed (Fig. 4). However, the P concentration gradient was not related to the relative compositions of hydrogenotrophs and acetotrophs to the degree that it was observed for the SO_4^{2-} gradient (e.g., between WCA-2A and WCA-3A). Thus, sulfate concentrations and the activities of SRPs appear to be the most dominant controllers of the methanogenic pathway in the WCAs of Everglades.

SRPs are important coinhabitants with methanogens (12, 42, 52). Our qPCR results indicated that SRPs outnumbered methanogens in WCA-2A and revealed that their numbers were similar even in WCA-3A (Fig. 2). Even though WCA-2A has higher concentrations of SO_4^{2-} than many other freshwater marshes, such as

WCA-3A (Table 1), the SO_4^{2-} concentration may not be high enough to support such high numbers of SRPs relative to the numbers of methanogens in WCAs. In a recent study, we found that *dsrB* transcripts from syntrophic SRPs belonging to the *Syntrophobacterales* comprised ≥75% of total *dsrB* transcripts found in the soils of sites F1, U3, and W3 (52). F4 soils, which were not tested in the previous study, also showed similar proportions of syntrophs in the present work (76%) (see Fig. S6 in the supplemental material). The high proportion of syntrophic SRPs likely explains the relatively high number of SRPs that were observed in our studies.

In conclusion, the numbers of copies and structures of *dsrB* and *mcrA* and their respective activities vary with nutrient status in the water conservation areas of the Florida Everglades. Depending on the available SO_4^{2-} concentration, SRPs are involved in controlling the methanogenic pathways, shaping methanogen assemblage structure, and controlling the CH_4 emission rate and pathway.

ACKNOWLEDGMENTS

The present research was supported by a grant from the National Science Foundation (DEB 0841596) and funding from the Everglades Agricultural Area Environmental Protection District, the Florida Department of Environmental Protection, and the Florida Department of Agriculture and Consumer Services.

We thank Claire Langford for isotope analysis. We thank James Colee for assistance with statistical analysis.

REFERENCES

1. **Stephens JC.** 1956. Subsidence of organic soils in the Florida Everglades. Soil Sci Soc Am J **20:**77–80. http://dx.doi.org/10.2136/sssaj1956.03615995002000010019x.
2. **Anderson B, Bartlett K, Frolking S, Hayhoe K, Jenkins J, Salas W.** 2010. Methane and nitrous oxide emissions from natural sources, Environmental Protection Agency, Office of Atmospheric Programs, Washington, DC.
3. **Cicerone RJ, Oremland RS.** 1988. Biogeochemical aspects of atmospheric methane. Global Biogeochem Cycles **2:**299–327. http://dx.doi.org/10.1029/GB002i004p00299.
4. **Craft CB, Richardson CJ.** 1993. Peat accretion and phosphorus accumulation along a eutrophication gradient in the northern Everglades. Biogeochemistry **22:**133–156. http://dx.doi.org/10.1007/BF00002708.
5. **DeBusk WF, Reddy KR, Koch MS, Wang Y.** 1994. Spatial distribution of soil nutrients in a northern Everglades marsh: Water Conservation Area 2A. Soil Sci Soc Am J **58:**543–552. http://dx.doi.org/10.2136/sssaj1994.03615995005800020042x.
6. **Koch MS, Reddy KR.** 1992. Distribution of soil and plant nutrients along a trophic gradient in the Florida Everglades. Soil Sci Soc Am J **56:**1492–1499. http://dx.doi.org/10.2136/sssaj1992.03615995005600050026x.
7. **Reddy KR, DeLaune RD, DeBusk WF, Koch MS.** 1993. Long-term nutrient accumulation rates in the Everglades. Soil Sci Soc Am J **57:**1147–1155. http://dx.doi.org/10.2136/sssaj1993.03615995005700040044x.
8. **DeBusk WF, Reddy KR.** 1998. Turnover of detrital organic carbon in a nutrient impacted Everglades marsh. Soil Sci Soc Am J **62:**1460–1468. http://dx.doi.org/10.2136/sssaj1998.03615995006200050045x.
9. **Wright A, Reddy KR.** 2001. Heterotrophic microbial activities in northern Everglades wetland. Soil Sci Soc Am J **65:**1856–1864. http://dx.doi.org/10.2136/sssaj2001.1856.
10. **Castro HF, Ogram A, Reddy KR.** 2004. Phylogenetic characterization of methanogenic assemblages in eutrophic and oligotrophic areas of the Florida Everglades. Appl Environ Microbiol **70:**6559–6568. http://dx.doi.org/10.1128/AEM.70.11.6559-6568.2004.
11. **Chauhan A, Ogram A, Reddy KR.** 2004. Syntrophic-methanogenic associations along a nutrient gradient in the Florida Everglades. Appl Environ Microbiol **70:**3475–3484. http://dx.doi.org/10.1128/AEM.70.6.3475-3484.2004.
12. **Drake HL, Aumen NG, Kuhner C, Wagner C, Grieshammer A, Schmittroth M.** 1996. Anaerobic microflora of Everglades sediments effects of nutrients on population profiles and activities. Appl Environ Microbiol **62:**486–493.
13. **Conrad R.** 1999. Contribution of hydrogen to methane production and control of hydrogen concentrations in methanogenic soils and sediments. FEMS Microbiol Ecol **28:**193–202. http://dx.doi.org/10.1111/j.1574-6941.1999.tb00575.x.
14. **Holmes ME, Chanton JP, Bae H-S, Ogram A.** 2014. Effect of nutrient enrichment on $\delta^{13}CH_4$ and the methane production pathway in the Florida Everglades. J Geophys Res Biogeosci **119:**1267–1280. http://dx.doi.org/10.1002/jgrg.20122.
15. **Chasar LS, Chanton JP, Glaser PH, Siegel DI, Rivers JS.** 2000. Radiocarbon and stable carbon isotopic evidence for transport and transformation of dissolved organic carbon, dissolved inorganic carbon, and CH_4 in a northern Minnesota peatland. Global Biogeochem Cycles **14:**1095–1108. http://dx.doi.org/10.1029/1999GB001221.
16. **Chan OC, Claus P, Casper P, Ulrich A, Lueders T, Conrad R.** 2005. Vertical distribution of structure and function of the methanogenic archaeal community in Lake Dagow sediment. Environ Microbiol **7:**1139–1149. http://dx.doi.org/10.1111/j.1462-2920.2005.00790.x.
17. **Jaatinen K, Fritze H, Laine J, Laiho R.** 2007. Effects of short- and long-term water-level drawdown on the populations and activity of aerobic decomposers in a boreal peatland. Glob Chang Biol **13:**491–510. http://dx.doi.org/10.1111/j.1365-2486.2006.01312.x.
18. **Keller JK, Bridgham SD.** 2007. Pathways of anaerobic carbon cycling across an ombrotrophic-minerotrophic peatland gradient. Limnol Oceanogr **52:**96–107. http://dx.doi.org/10.4319/lo.2007.52.1.0096.
19. **Kotsyurbenko OR, Friedrich AW, Simankova MV, Nozhevnikova AN, Golyshin PN, Timmis KN, Conrad R.** 2007. Shift from acetoclastic to H_2-dependent methanogenesis in a West Siberian peat bog at low pH values and isolation of an acidophilic Methanobacterium strain. Appl Environ Microbiol **73:**2344–2348. http://dx.doi.org/10.1128/AEM.02413-06.
20. **Yavitt JB, Seidman-Zager M.** 2006. Methanogenic conditions in northern peat soils. Geomicrobiol J **23:**119–127.
21. **Hines ME, Duddleston KN, Rooney-Varga JN, Fields D, Chanton JP.** 2008. Uncoupling of acetate degradation from methane formation in Alaskan wetlands: connections to vegetation distribution. Global Biogeochem Cycles **22:**GB2017.
22. **Kuivila KM, Murray JW, Devol AH.** 1990. Methane production in the sulfate-depleted sediments of two marine basins. Geochim Cosmochim Acta **54:**403–411. http://dx.doi.org/10.1016/0016-7037(90)90329-J.
23. **Oremland RS, Marsh LM, Polcin S.** 1982. Methane production and simultaneous sulfate reduction in anoxic salt marsh sediments. Nature **296:**143–145. http://dx.doi.org/10.1038/296143a0.
24. **Lovley DR, Klug MJ.** 1983. Sulfate reducers can outcompete methanogens at freshwater sulfate concentrations. Appl Environ Microbiol **45:**187–192.
25. **Winfrey MR, Zeikus JG.** 1977. Effect of sulfate on carbon and electron flow during microbial methanogenesis in freshwater sediments. Appl Environ Microbiol **33:**275–281.
26. **Oude Elferink SJWH, Visser A, Hulshoff-Pol LW, Stams AJM.** 1994. Sulfate reduction in methanogenic bioreactors. FEMS Microbiol Rev **15:**119–136. http://dx.doi.org/10.1111/j.1574-6976.1994.tb00130.x.
27. **Bryant MP, Campbell LL, Reddy CA, Crabill MR.** 1977. Growth of *Desulfovibrio* in lactate or ethanol media low in sulfate in association with H_2-utilizing methanogenic bacteria. Appl Environ Microbiol **33:**1162–1169.
28. **McInerney MJ, Struchtemeyer CG, Sieber J, Mouttaki H, Stams AJM, Schink B, Rohlin L, Gunsalus RP.** 2008. Physiology, ecology, phylogeny, and genomics of microorganisms capable of syntrophic metabolism. Ann N Y Acad Sci **1125:**58–72. http://dx.doi.org/10.1196/annals.1419.005.
29. **Orem W, Gilmour C, Axelrad D, Krabbenhoft D, Scheidt D, Kalla P, McCormick P, Gabriel M, Aiken G.** 2011. Sulfur in the South Florida ecosystem: distribution, sources, biogeochemistry, impacts, and management for restoration. Crit Rev Environ Sci Technol **41**(Suppl 1)**:**249–288. http://dx.doi.org/10.1080/10643389.2010.531201.
30. **Steinberg LM, Regan JM.** 2008. Phylogenetic comparison of the methanogenic communities from an acidic, oligotrophic fen and an anaerobic digester treating municipal wastewater sludge. Appl Environ Microbiol **74:**6663–6671. http://dx.doi.org/10.1128/AEM.00553-08.
31. **Foti M, Sorokin DY, Lomans B, Mussman M, Zacharova EE, Pimenov NV, Kuenen JG, Muyzer G.** 2007. Diversity, activity, and abundance of

sulfate-reducing bacteria in saline and hypersaline soda lakes. Appl Environ Microbiol **73:**2093–2100. http://dx.doi.org/10.1128/AEM.02622-06.
32. **Hall TA.** 1999. BioEdit: a user-friendly biological sequence alignment editor and analysis program for Windows 95/98/NT. Nucleic Acids Symp Ser **41:**95–98.
33. **Thompson JD, Gibson TJ, Plewniak F, Jeanmougin F, Higgins DG.** 1997. The Clustal_X Windows interface: flexible strategies for multiple sequence alignment aided by quality analysis tools. Nucleic Acids Res **25:**4876–4882. http://dx.doi.org/10.1093/nar/25.24.4876.
34. **Tamura K, Peterson D, Peterson N, Stecher G, Nei M, Kumar S.** 2011. MEGA5: molecular evolutionary genetics analysis using maximum likelihood, evolutionary distance, and maximum parsimony methods. Mol Biol Evol **28:**2731–2739. http://dx.doi.org/10.1093/molbev/msr121.
35. **Schloss PD, Westcott SL, Ryabin T, Hall JR, Hartmann M, Hollister EB, Lesniewski RA, Oakley B, Parks DH, Robinson CJ, Sahl JW, Stres B, Thallinger GG, Van Horn DJ, Weber CF.** 2009. Introducing mothur: open-source, platform-independent, community-supported software for describing and comparing microbial communities. Appl Environ Microbiol **75:**7537–7541. http://dx.doi.org/10.1128/AEM.01541-09.
36. **Hamady M, Lozupone C, Knight R.** 2010. Fast UniFrac: facilitating high-throughput phylogenetic analyses of microbial communities including analysis of pyrosequencing and PhyloChip data. ISME J **4:**17–27. http://dx.doi.org/10.1038/ismej.2009.97.
37. **Martin AP.** 2002. Phylogenetic approaches for describing and comparing the diversity of microbial communities. Appl Environ Microbiol **68:**3673–3682. http://dx.doi.org/10.1128/AEM.68.8.3673-3682.2002.
38. **Lozupone C, Knight R.** 2005. UniFrac: a new phylogenetic method for comparing microbial communities. Appl Environ Microbiol **71:**8228–8235. http://dx.doi.org/10.1128/AEM.71.12.8228-8235.2005.
39. **Steinberg LM, Regan JM.** 2009. *mcrA*-targeted real-time quantitative PCR method to examine methanogen communities. Appl Environ Microbiol **75:**4435–4442. http://dx.doi.org/10.1128/AEM.02858-08.
40. **Meier J, Voigt A, Babenzien HD.** 2000. A comparison of $^{35}S\text{-}SO_4^{2-}$ radiotracer techniques to determine sulphate reduction rates in laminated sediments. J Microbiol Methods **41:**9–18. http://dx.doi.org/10.1016/S0167-7012(00)00144-5.
41. **Ulrich GA, Krumholz LR, Suflita JM.** 1997. A rapid and simple method for estimating sulfate reduction activity and quantifying inorganic sulfides. Appl Environ Microbiol **63:**1627–1630.
42. **Castro H, Reddy KR, Ogram A.** 2002. Composition and function of sulfate-reducing prokaryotes in eutrophic and pristine areas of the Florida Everglades. Appl Environ Microbiol **68:**6129–6137. http://dx.doi.org/10.1128/AEM.68.12.6129-6137.2002.
43. **Fossing H, Jørgensen BB.** 1989. Measurement of bacterial sulfate reduction in sediments: evaluation of a single-step chromium reduction method. Biogeochemistry **8:**205–222.
44. **Hori T, Sasaki D, Haruta S, Shigematsu T, Ueno Y, Ishii M, Lgarashi Y.** 2011. Detection of active, potentially acetate-oxidizing syntrophs in an anaerobic digester by flux measurement and formyltetrahydrofolate synthetase (FTHFS) expression profiling. Microbiology **157:**1980–1989. http://dx.doi.org/10.1099/mic.0.049189-0.
45. **White JR, Reddy KR.** 1999. Influence of nitrate and phosphorus loading on denitrifying enzyme activity in Everglades wetland soils. Soil Sci Soc Am J **63:**1945–1954. http://dx.doi.org/10.2136/sssaj1999.6361945x.
46. **Sanders R.** 2015. Compilation of Henry's law constants (version 4.0) for water as solvent. Atmos Chem Phys **15:**4399–4981.
47. **Albert DB, Martens CS.** 1997. Determination of low-molecular weight organic acid concentrations in seawater and pore-water samples via HPLC. Mar Chem **56:**27–37. http://dx.doi.org/10.1016/S0304-4203(96)00083-7.
48. **Merritt DA, Hayes JM, Marias DJD.** 1995. Carbon isotopic analysis of atmospheric methane by isotope-ratio-monitoring gas chromatography mass-spectrometry. J Geophys Res **100:**1317–1326. http://dx.doi.org/10.1029/94JD02689.
49. **ter Braak CJF, Šmilauer P.** 2002. CANOCO reference manual and CanoDraw for Windows user's guide: software for canonical community ordination (version 4.5). Microcomputer Power, Ithaca, NY.
50. **Reddy KR, White JR, Wright A, Chua T.** 1999. Influence of phosphorus loading on microbial processes in the soil and water column of wetlands, p 249–273. *In* Reddy KR, O'Connor GA, Schelske CL (ed), Phosphorus biogeochemistry in subtropical ecosystems. Lewis Publishers, New York, NY.
51. **Castro H, Newman S, Reddy KR, Ogram A.** 2005. Distribution and stability of sulfate-reducing prokaryotic and hydrogenotrophic methanogenic assemblages in nutrient-impacted regions of the Florida Everglades. Appl Environ Microbiol **71:**2695–2704. http://dx.doi.org/10.1128/AEM.71.5.2695-2704.2005.
52. **Bae HS, Dierberg FE, Ogram A.** 2014. Syntrophs dominate sequences associated with the mercury methylation-related gene hgcA in the water conservation areas of the Florida Everglades. Appl Environ Microbiol **80:**6517–6526. http://dx.doi.org/10.1128/AEM.01666-14.
53. **Dridi B, Fardeau ML, Ollivier B, Raoult D, Drancourt M.** 2012. *Methanomassiliicoccus luminyensis* gen. nov., sp. nov., a methanogenic archaeon isolated from human faeces. Int J Syst Evol Microbiol **62:**1902–1907. http://dx.doi.org/10.1099/ijs.0.033712-0.
54. **Borrel G, Harris HMB, Tottey W, Mihajlovski A, Parisot N, Peyretaillade E, Peyret P, O'Toole PW, Brugere JF.** 2012. Genome sequence of "*Candidatus* Methanomethylophilus alvus" Mx1201, a methanogenic archaea from the human gut belonging to a seventh order of methanogens. J Bacteriol **194:**6944–6945. http://dx.doi.org/10.1128/JB.01867-12.
55. **Lueders T, Chin K-J, Conrad R, Friedrich M.** 2001. Molecular analyses of methyl-coenzyme M reductase alphasubunit (*mcrA*) gene in rice field soil and enrichment cultures reveal the methanogenic phenotype of a novel archaeal lineage. Environ Microbiol **3:**194–204. http://dx.doi.org/10.1046/j.1462-2920.2001.00179.x.
56. **Whiticar MJ.** 1999. Carbon and hydrogen isotope systematics of bacterial formation and oxidation of methanes. Chem Geol **161:**291–314. http://dx.doi.org/10.1016/S0009-2541(99)00092-3.
57. **Conrad R.** 2005. Quantification of methanogenic pathways using stable carbon isotopic signatures: a review and a proposal. Org Geochem **36:**739–752. http://dx.doi.org/10.1016/j.orggeochem.2004.09.006.
58. **Vaithiyanathan P, Richardson CJ.** 1997. Nutrient profiles in the Everglades: examination along the eutrophication gradient. Sci Total Environ **205:**81–95. http://dx.doi.org/10.1016/S0048-9697(97)00191-5.
59. **Galand PE, Fritze H, Conrad R, Yrjala K.** 2005. Pathways for methanogenesis and diversity of methanogenic Archaea in three boreal peatland ecosystems. Appl Environ Microbiol **71:**2195–2198. http://dx.doi.org/10.1128/AEM.71.4.2195-2198.2005.
60. **Galand PE, Saarnio S, Fritze H, Yrjala K.** 2002. Depth related diversity of methanogen archaea in Finnish oligotrophic fen. FEMS Microbiol Ecol **42:**441–449. http://dx.doi.org/10.1111/j.1574-6941.2002.tb01033.x.
61. **Jetten MSM, Stams AJM, Zehnder AJB.** 1992. Methanogenesis from acetate—a comparison of the acetate metabolism in *Methanothrix soehngenii* and *Methanosarcina* spp. FEMS Microbiol Lett **88:**181–197. http://dx.doi.org/10.1111/j.1574-6968.1992.tb04987.x.
62. **Hedderich R, Whitman W.** 2006. Physiology and biochemistry of the methane-producing Archaea, p 1050–1079. *In* Dworkin M, Falkow S, Rosenberg E, Schleifer K-H, Stackebrandt E (ed), The prokaryotes, 3rd ed, vol 2. Springer Verlag, New York, NY.
63. **Garcia J-L, Ollivier B, Whitman W.** 2006. The order Methanomicrobiales, p 208–230. *In* Dworkin M, Falkow S, Rosenberg E, Schleifer K-H, Stackebrandt E (ed), The prokaryotes, 3rd ed, vol 3. Springer Verlag, New York, NY.
64. **Schönheit P, Kristjansson JK, Thauer RK.** 1982. Kinetic mechanism for the ability of sulphate reducers to out-compete methanogens for acetate. Arch Microbiol **132:**285–288. http://dx.doi.org/10.1007/BF00407967.
65. **Hornibrook ERC, Longstaffe FJ, Eyfe WS.** 2000. Evolution of stable isotope compositions for methane and carbon dioxide in freshwater wetlands and other anaerobic environments. Geochim Cosmochim Acta **64:**1013–1027. http://dx.doi.org/10.1016/S0016-7037(99)00321-X.
66. **Whiticar MJ, Faber E, Schoell M.** 1986. Biogenic methane formation in marine and freshwater environments: CO_2 reduction vs. acetate fermentation—isotope evidence. Geochim Cosmochim Acta **50:**693–709. http://dx.doi.org/10.1016/0016-7037(86)90346-7.
67. **Wu WM, Hickey RF, Zeikus JG.** 1991. Characterization of metabolic performance of methanogenic granules treating brewery wastewater: role of sulfate-reducing bacteria. Appl Environ Microbiol **57:**3438–3449.
68. **Holmes ME, Chanton J, Tfaily M, Ogram A.** 2015. CO_2 and CH_4 isotope compositions and production pathways in a tropical peatland. Global Biogeochem Cycles **29:**1–18. http://dx.doi.org/10.1002/2014GB004951.